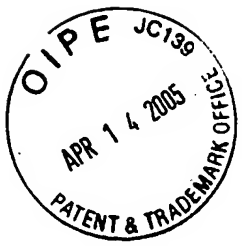

IN THE UNITED STATES PATENT AND TRADEMARK OFFICE

In re Patent Application of

BEGUIN et al. Atty. Ref.: 1721-84

Appl. No. 10/523,397 TC/A.U. Unassigned

371 US national phase of PCT/FR03/002499

Filed: February 3, 2005 Examiner: Unassigned

For: METHOD FOR OPENING CARBON NANOTUBES AT THE ENDS THEREOF AND IMPLEMENTATION

* * * * * * * * * * * *

April 14, 2005

Commissioner for Patents
P.O. Box 1450
Alexandria, VA 22313-1450

Sir:

SUPPLEMENTAL SUBMISSION

Supplemental to the Transmittal of April 8, 2005, attached is a copy of the further Smith et al (Carbon 41 (2003) 1221-1230) reference listed in the International Search Report and listed on the PTO 1449 Form filed February 3, 2005. Return of an initialed copy of the PTO 1449 Form, pursuant to MPEP § 609, is requested.

Respectfully submitted,

NIXON & VANDERHYE P.C.

By: _____
B. J. Sadoff
Reg. No. 36,663

BJS:
1100 North Glebe Road, 8th Floor
Arlington, VA 22201-4714
Telephone: (703) 816-4000
Facsimile: (703) 816-4100

PERGAMON

Carbon 41 (2003) 1221–1230

CARBON

Selective oxidation of single-walled carbon nanotubes using carbon dioxide

Milton R. Smith Jr.[a], Sheila W. Hedges[a], Robert LaCount[b], Douglas Kern[b], Naresh Shah[c], Gerald P. Huffman[c], Bradley Bockrath[a,*]

[a]National Energy Technology Laboratory, US Department of Energy, P.O. Box 10940, Pittsburgh, PA 15236, USA
[b]Virolac Industries, 403 Arbor Court, Waynesburg, PA 15370, USA
[c]University of Kentucky, 533 South Limestone Street, Room 111, Lexington, KY 40508-4005, USA

Received 1 October 2002; accepted 25 January 2003

Abstract

A simple process for selective removal of carbon from single-walled carbon nanotube samples was developed based on a mild oxidation by carbon dioxide. The reactivity profiles of as prepared and purified nanotube samples were determined using both TG and a related analytical technique, controlled atmosphere programmed temperature oxidation (CAPTO). The complex differential rate curves for weight loss (DTG) or carbon dioxide evolution (CAPTO) could be resolved by a series of Gaussian peaks each associated with carbonaceous species of different reactivity. Comparisons were made between samples as received after preparation by the laser ablation method, after purification by nitric acid oxidation, and both of these after reaction with CO_2. The DTG of as prepared tubes had a broad major peak centered about 410 °C. Mild oxidation of as prepared nanotubes under flowing carbon dioxide at 600 °C preferentially removed more reactive carbon species leaving behind a narrower distribution about the major peak in DTG. In contrast to the as prepared material, the sample that had been purified using nitric acid had a more distinct separation of the major DTG peaks between more and less readily oxidized material. Oxidation of this sample with CO_2 selectively removed the peak associated with the most readily oxidized material. The original CO_2 oxidation experiments performed on the analytical scale were successfully scaled up to a small preparative scale.
Published by Elsevier Science Ltd.

Keywords: A. Carbon nanotubes; B. Oxidation; C. Thermal analysis (DTG and TGA); D. Reactivity

1. Introduction

Partial and selective oxidation has been routinely used to modify the adsorption characteristics of activated carbons. Similar approaches might be valuable in modifying single-walled carbon nanotubes (SWCNTs). In particular, it has already been demonstrated that partial oxidation with carbon dioxide opens the ends of and "thins" multi-walled nanotubes [1] as well as increases the microporosity of soot [2] derived from arc vaporization of carbon. In fact, we have discovered that mild oxidation with CO_2 is an effective way for activating SWCNTs, thereby increasing their hydrogen storage capacity [3]. In addition to activating SWCNTs, mild CO_2 oxidation provides insight into their chemical reactivity and character. The application of thermogravimetry (TG) and related techniques is particularly valuable in this context. A comparison between samples of raw and purified nanotubes received from tubes@rice [4] is the main focus of this work. The raw material was purified by partial oxidation using HNO_3 followed by extraction and washing [5]. This technique was devised to generate high-purity SWCNTs by removing the commonly encountered contaminants: metallic catalyst, amorphous carbon, "shells", and various fullerite structures. A recent extensive transmission electron microscopy (TEM) study of the effects of purification by treatment with strong acids has shown that typically employed purification procedures lead to partial oxidation of SWCNTs themselves and sometimes to an extensive disruption of the tubular structure [6]. We report below on the use of carbon dioxide for the selective removal of

*Corresponding author.
E-mail address: bockrath@netl.doe.gov (B. Bockrath).

0008-6223/03/$ – see front matter Published by Elsevier Science Ltd.
doi:10.1016/S0008-6223(03)00054-X

easily oxidized material from SWCNTs produced by the laser ablation method [7] and purified samples of those materials [5].

2. Experimental

SWCNT samples were purchased from tubes@rice. The "Purified" grade was received as a suspension in toluene (6 mg/ml). Samples (typically 10 ml) were withdrawn and evaporated in a stream of N_2 and then heated to 110 °C at 25 mmHg pressure for 2 h or at 140 °C for 12 h at atmospheric pressure (1 mmHg=133.322 Pa). Samples were often stored under ambient conditions for days prior to use and most received moderate grinding prior to use. "Raw Material" grade was received as a solid fibrous material and was subjected to moderate grinding to facilitate handling. Submicron nickel powder was purchased from Aldrich. Huffman Laboratories performed the direct determination of the oxygen content of the nanotubes. The amount of CO and CO_2 formed during pyrolysis to 1200 °C was determined in a Leco RO-478 oxygen analyzer.

2.1. Carbon dioxide oxidation

In a typical experiment, 60–200 mg of SWCNT was placed between loose quartz wool plugs in a 20 cm×12 mm Vycor tube. This tube was placed inside a 1 in. O.D. quartz tube in a tube furnace (1 in.=2.54 cm). The inner tube was connected to a gas manifold via PTFE fittings and a flow of dry argon was begun through the sample at 10 ml/min. Carbon dioxide was then added to bring the total flow to 20 ml/min. The sample was brought to about 600 °C over the course of about 1 h while the effluent was monitored by mass spectrometry. After about 2 h at 600 °C, the furnace was turned off and the sample was cooled to ambient temperature under an Ar flow. A typical recovery was 68–69% (w/w) for both the purified and raw samples.

2.2. Controlled atmosphere programmed temperature oxidation (CAPTO) analysis

CAPTO analyses were performed by Virolac Industries (Waynesburg, PA, USA). The general method has been described [8]. Briefly, the ground sample (10–15 mg) was well dispersed in 12 g of WO_3, added as a diluent, and packed into a quartz tube. The WO_3 was heated under O_2 to 1050 °C before use to eliminate potential interferences due to trace organic contamination. A thermocouple located within the bed read the actual temperature of the sample. A stream of pure oxygen regulated by a mass flow controller at 100 ml/min was passed through the sample plug while it was heated using a programmed temperature ramp of 3 °C/min up to 1050 °C. Complete combustion of the gases exiting the primary reactor was obtained in a secondary catalytic reactor held at 1050 °C. A calibrated Fourier transform (FT) IR spectrometer determined the carbon dioxide content of the exit stream, and the data was plotted as the mass of carbon dioxide evolved as a function of sample temperature. These plots were analyzed by a commercial peak-fitting software package or in some cases by using MS Excel as described below.

2.3. Thermal analysis

Nanotube samples (~2–3 mg) were placed in the platinum pan of a Perkin-Elmer Model TG-7 TG system. Submicron Ni samples used to emulate the oxidation of catalyst particles were about 7 mg. Each type of sample was subjected to at least duplicate TG scans. The temperature was increased at 5 °C/min. from ambient to 1000 °C. Reactive gas flow, either air or carbon dioxide, was 50 ml/min. The data files were written to a disc and opened with MS Excel. The first derivative of the thermal curves was calculated numerically from a 10-point moving average of the mass and temperature over a 5 °C range.

Most DTG (derivative thermogravimetry) curves were analyzed using multiple Gaussian curves of the form:

$$y_i = y_{(\min)} \exp\left[-4 \ln 2 (T_i - T_{y(\min)})^2 / \mathrm{HfWdth}^2\right]$$

generated in MS Excel. Values of y_i were generated for approximately 1600 points between i=30 °C and 1000 °C, where $y_{(\min)}$ is the maximum rate of mass change at $T_{y(\min)}$ and HfWdth represents the half width of the Gaussian curve. CAPTO curves and the DTG in air of carbon dioxide oxidized material were better fit by a log normal function instead of the simpler Gaussian curves. The log normal function was of the form described by Billo [9] but modified to include asymmetry before and after the extremum. The contributions of each of the identifiable steps was made by integrating the curves generated from a non-linear least squares fit obtained by using the add-in "Solver" within Excel. Adjustable parameters were peak height, half width, temperature at the maximum, and two adjustable asymmetry factors for the log normal functions. The minimum number of curves was used to fit each DTG. This was determined by increasing their number until the Pearson R^2 value was not significantly improved. In one case (Fig. 5) Solver was not used because the non-zero baseline of the DTG curve caused it to add very broad Gaussian peaks. Instead, six Gaussian functions were fitted manually and refined stepwise until the fit was judged visually adequate (R^2=0.993). The areas under the individual peaks are given as the percentage of the mass loss for TG or the percentage of total carbon dioxide formed for CAPTO.

2.4. High-resolution (HR) TEM

Samples of raw material grade and purified grade

SWCNT before and after CO_2 oxidation were also examined by HRTEM at The University of Kentucky. TEM samples were prepared by suspending about 1 mg SWCNT sample in 5 ml acetone. The suspension was ultrasonicated for over 30 min to separate out the bundles. One drop of the supernatant liquid (transparent looking by naked eye) was placed on a lacey carbon grid. A Jeol 2010F TEM system was operated at 200 kV accelerating voltage. Digital images were captured by Gatan CCD camera and software.

3. Results and discussion

3.1. Rice-purified SWCNTs

CAPTO analysis of purified-grade rice SWCNTs is shown in Fig. 1. The weight of carbon evolved as carbon dioxide is plotted versus temperature. The curve shows that the initial oxidation starting at 200 °C is the first of four distinguishable but unresolved peaks. The results of curve fitting ($R^2 = 0.999$) and integration of the individual components are also shown. The first oxidation is centered at 297 °C and accounts for 28% of the total. The major component (67%) is centered at 368 °C and two minor components at 409 °C (1%) and 459 °C (5%) follow it.

One concern about TG and related methods is the possibility of distortion caused by the effects of local heating from exothermic reactions. In fact, it has been reported that local heating caused by oxidation of amorphous carbon leads to the pre-ignition of SWCNTs [4,13]. The CAPTO method was expressly designed [8] to minimize exothermic effects by providing a large thermal mass though the heavy dilution (1200:1) of the sample with WO_3. This ratio was selected in the original development of the method based on results of a progressive dilution of the sample. The effect of exothermic reactions was progressively reduced with greater dilution until they were extinguished before reaching the ratios used here. The use of an even higher dilution had no effect on the result. Thus, CAPTO of purified-rice SWCNTs using a 4000:1 dilution gave a curve practically identical to that in Fig. 1, except for scale of the response. Additional experiments were performed substituting quartz fibers or Celite for WO_3 to rule out the possibility that it might act as an oxidation catalyst. The fundamental aspects of the curves did not change indicating that catalysis by the diluent was not a factor.

Typical TG and DTG curves for purified SWCNTs are shown in Fig. 2. Similarities and differences between CAPTO (based on carbon dioxide evolution) and TG (based on mass loss) are evident. First, TG shows a mass loss of 3.2% occurs before 150 °C that is probably due to water that had been picked up from ambient air before the test. In separate experiments, mass loss and mass spectrometry indicated that the SWCNT samples lost water (up to 8%, depending on sample history) under inert atmosphere at temperatures of 100–200 °C. Second, mass loss from oxidation begins at a higher temperature in TG (air) than in CAPTO (oxygen). In TG oxidation begins at about 270 °C and seems to occur in at least four distinct, but not well separated steps. The residue at 1000 °C amounted to 9.9% of the original mass, and is attributed to a mixture of cobalt and nickel oxides derived from the catalyst used in synthesizing the SWCNT [4]. Analysis of the residue by inductively coupled plasma (ICP) confirmed that it was made up of the oxides of these metals.

A search for local heating effects in TG was made using an approach similar to that done in CAPTO. Purified SWCNTs were ground and intimately mixed with 12 parts of WO_3. When compared to Fig. 2, the form of the DTG was unchanged although there was somewhat more noise because of the scant amount of carbon in the sample. Thus evidence for effects due to uncontrolled exothermic reactions is lacking in both TG and CAPTO.

The DTG curve (Fig. 3) reveals that the major oxidation reactions beginning at about 270 °C are readily distinguish-

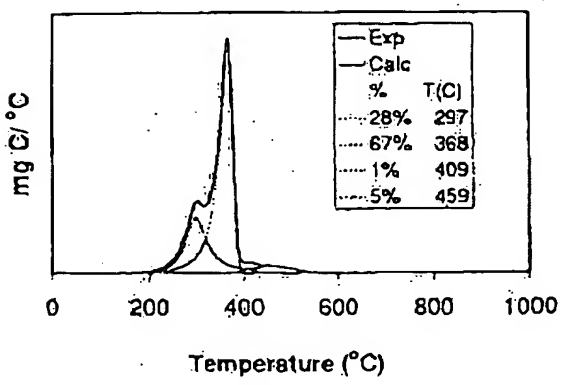

Fig. 1. Experimental and calculated CAPTO purified rice nanotubes in oxygen.

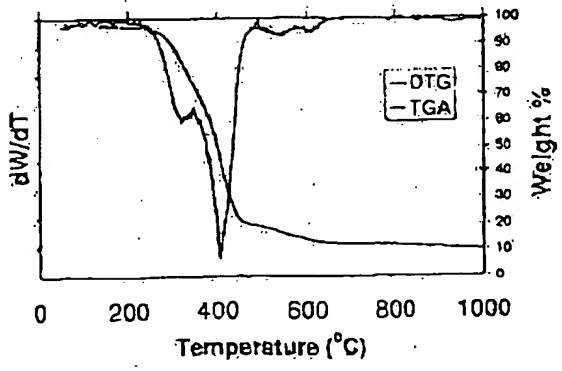

Fig. 2. TG and DTG of purified rice nanotubes in air.

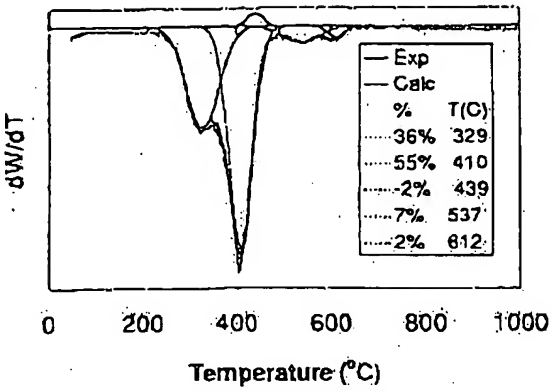

Fig. 3. Experimental and calculated DTG of purified rice nanotubes in air

able as at least two processes. The curve fits the data between 150 and 1000 °C well (R^2=0.997). The low temperature oxidation reaches a maximum rate at 329 °C and accounts for 36% of the total mass loss between the end of water evolution and 1000 °C. The main peak at 410 °C accounts for 55% of the mass change and the high temperature peaks at 537 and 612 °C account for 7 and 2%, respectively. The remaining mass loss is indistinct in the derivative curve.

An arbitrary positive Gaussian curve was added to the calculated DTG curve to account for the mass gain associated with the oxidation of the catalytic metals. The central temperature, half width, and peak height were allowed to vary, but the mass gain (2%) for oxide formation was set by assuming an equi-atomic Co/Ni alloy was oxidized to the +2 state. The final refinement placed its center at 439 °C. Evidence that inclusion of this peak is reasonable was obtained from TG of a sample of pure nickel metal of sub-micron particle size. Oxidation of this nickel sample to NiO (98.7% of theory) took place between 350 and 600 °C.

The oxidation using both air (TG) and oxygen (CAPTO) indicates two major constituents are present in the purified nanotube sample, but neither technique could fully resolve them. A less reactive but possibly more selective oxidant was chosen in an attempt to improve the resolution. Thus TG was performed on the purified rice sample in an atmosphere of carbon dioxide (Fig. 4). There are two major and easily distinguished mass losses, one between 200 and 600 °C (32%), the other between 650 and 950 °C (52%).

A good fit of the experimental DTG curve required a minimum of five peaks for carbon (Fig. 5). Significantly, the first peak is resolved from the others and accounts for roughly the same percentage of carbon (33%) as the leading peak in the DTG under air (36%) and in CAPTO (28%). Thus the first major peak seems to be a common element in all three techniques. Other similarities are

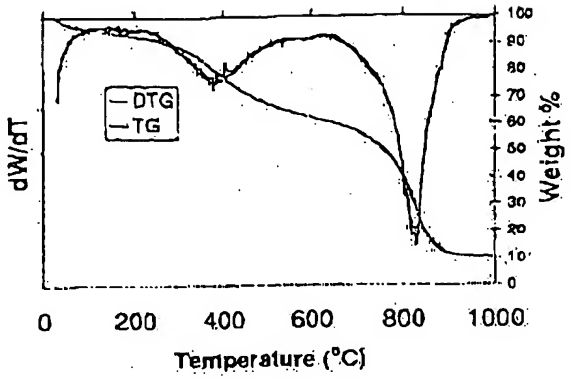

Fig. 4. TG and DTG of purified rice nanotubes in CO_2.

apparent. The loss from 30 to 200 °C (6%), due mostly to water, and the mass remaining at the end (10.3%), were comparable to those found earlier. As before, the gain due to oxidation of metals was accounted for by including a mass increase (2%) based on the theoretical amount expected. This contribution refined to the weight gain centered at 811 °C. This correlates reasonably well with the oxidation of a sample of pure submicron Ni in carbon dioxide that began at about 600 °C and reached a maximum rate at 885 °C. The ultimate gain corresponded to 98% of the theoretical amount for NiO.

3.2. Carbon dioxide oxidized purified grade SWCNTs

The analytical results described above provided reason to believe that a selective removal of the most easily oxidized carbon could be accomplished on a larger scale. Accordingly, the advantage of endothermic oxidation by carbon dioxide was carried from the analytical to a small preparative scale in a tube furnace. Samples of purified rice nanotubes were placed in a quartz tube and heated to 610 °C for about 2 h under a flow of 50% carbon dioxide

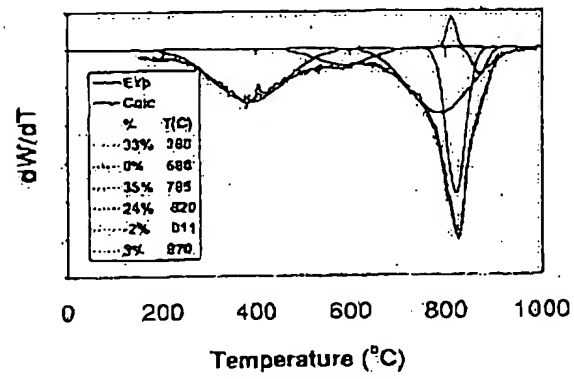

Fig. 5. Experimental and calculated DTG of purified rice nanotubes in CO_2.

in argon. The reaction was monitored by mass spectrometry. As the temperature increased a marked increase in the m/e 28 peak in the mass spectrum of the effluent was observed, as expected from the reaction:

$$CO_2 + C \rightarrow 2CO$$

After 1.6 h, this signal returned to the baseline associated with the mass fragment derived from the flow of carbon dioxide. In replicate experiments with varying sample sizes, 55–68% of the original sample weight was recovered after oxidation.

A 10-mg portion of the CO_2 oxidized purified rice material was subjected to CAPTO analysis in oxygen as shown in Fig. 6. The data were best fit ($R^2 = 0.999$) by four functions, the two at lower temperatures being asymmetric. The major contributor is centered at 383 °C (88%) with the remainder at small peaks at 324 °C (5%), 409 °C (1%), and 459 °C (5%). Comparison to Fig. 1 shows that the leading peak has been largely removed by CO_2 oxidation.

The corresponding TG of this material is shown in Fig. 7. A mass loss of 2% is centered at 94 °C (water) followed by the prominent and sharp oxidation reaching a maximum rate at 421 °C. Contributions to the curve above 150 °C were centered at 421 °C (84%), 498 °C (10%), and 625 °C (5%). Again, by comparison with Fig. 3, it is apparent that the leading peak has been removed.

For a closer comparison, Fig. 8 shows the overlay of DTG curves for a purified SWCNT before and after carbon dioxide oxidization (note derivative scale difference). The selective removal of the lower temperature constituents that was achieved by carbon dioxide oxidation is apparent. The major component is slightly shifted (11 °C) to higher temperature. This may be the result of increased order produced by the annealing effect of prolonged periods above 600 °C. Annealing of the rope-like structures by heating to similar temperatures has been reported [5]. A similar increase (15 °C) is seen when the corresponding

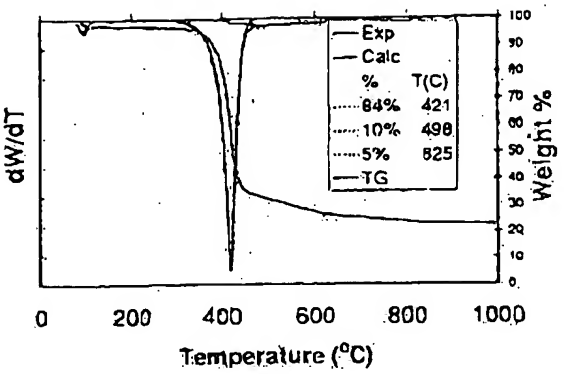

Fig. 7. TG and experimental and calculated DTG in air of a CO_2 oxidized purified rice SWCNT.

CAPTO curves are compared. The single main peak in both CAPTO (Fig. 6) or TG (Fig. 7) is evidence that the recovered material is relatively homogeneous.

Comparison of the CAPTO and DTG analyses shows that the onset of oxidation progresses toward higher temperatures as the reactivity of the oxidant decreases as expected. It begins about 200 °C in pure oxygen, is delayed until 270 °C in air, and does not begin until 300 °C in carbon dioxide. Oxidation by carbon dioxide is the most selective of the three and the most reactive component is well separated from the others. Significantly, the lower temperature oxidation peak accounts for 28–36% of the purified rice nanotubes in each analysis. The bulk of the remaining material is accounted for by peaks centered at 368 °C (oxygen) and 410 °C (air). In accord with its more selective nature, the high temperature envelope under carbon dioxide was resolved by two major components at 750 °C (35%) and 822 °C (24%) and a minor peak at 870 °C. These three analyses all reflect the fact that nitric acid purified nanotubes still contain a mixture of carbon species of differing reactivity.

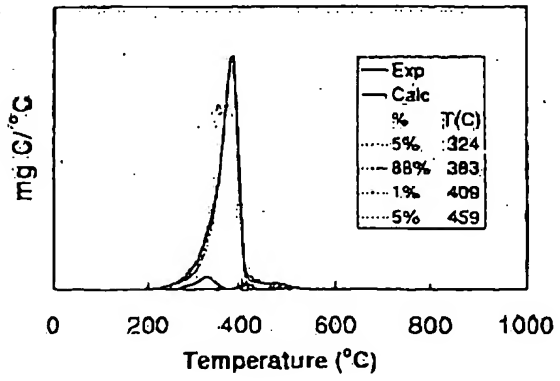

Fig. 6. Experimental and calculated CAPTO in oxygen of a CO_2 oxidized purified rice SWCNT.

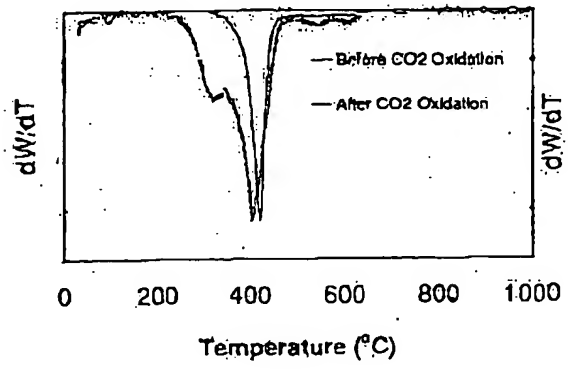

Fig. 8. DTG of a purified rice SWCNT in air before and after CO_2 oxidation.

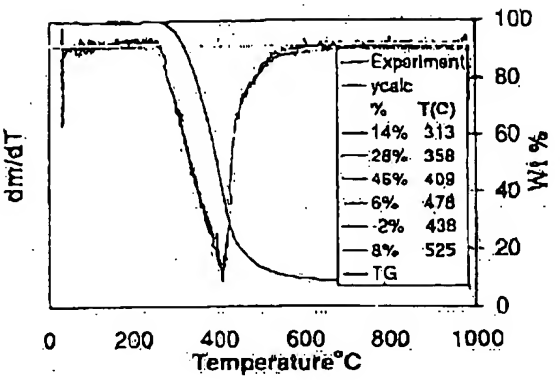

Fig. 9. TG and experimental and calculated DTG of rice raw material SWCNTs in air.

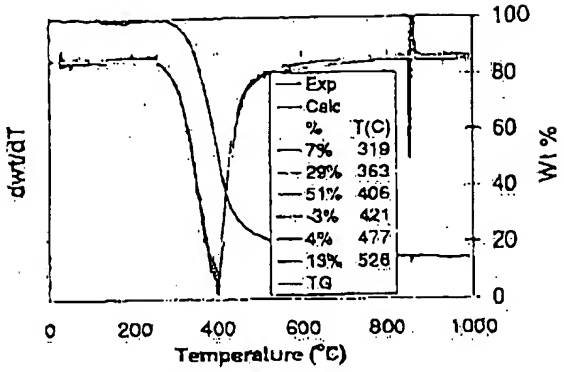

Fig. 10. TG and DTG of rice raw material after CO_2 oxidation.

3.3. Carbon dioxide oxidized raw material

The TG and DTG curves are given in Fig. 9. Weight loss in air started near 300 °C and continued to near 800 °C. After complete oxidation 7.3–8.8% Co/Ni oxides remained, corresponding to 5.8–6.9% of the metals in the sample. DTG reveals a complex pattern of oxidation losses that are well described ($R^2 = 0.996$) by a sum of Gaussian peaks at 313 °C (14%), 358 °C (28%), 409 °C (46%), 478 °C (6%), and 525 °C (8%). A peak for weight gain at 438 °C corresponds to metal oxidation.

Compared to purified grade, raw material began to oxidize at a higher temperature and required a set of more closely spaced Gaussian peaks for an adequate fit. Significantly, the major component of both samples is centered about 410 °C. By comparison of Figs. 3 and 9 it is evident that after purification the main component was a somewhat larger fraction of the total carbon. We also note that after purification the first two peaks found in the raw material are replaced by a single peak.

If the peak around 410 °C is due to nanotubes the material that comes before it must be assigned to forms of carbon that are more readily oxidized. For the raw material the first carbon peak is reasonably assigned to amorphous carbon. This assignment has been made in a study of SWCNTs made by the arc discharge method [10]. For the purified sample the first peak is likely to include nanotube fragments or badly damaged nanotubes introduced during the HNO_3 oxidation. Disruption of the nanotube structure and the introduction of a relatively high number of functional groups would make these fragments prone to easier oxidation. In support of this idea, we note that partially damaged nanotubes containing many defects have been observed in the purified material by HRTEM [6]. Similar findings were made with SWCNTs purified by oxidation in aqueous H_2O_2 [11]. In this case, amorphous carbon particles that coated the surface of nanotubes in the oxidized sample were removed by treatment with NaOH.

A comparison between the raw material before and after CO_2 oxidation was made next. The oxidation was carried out at 600 °C for 2 h just as with the purified sample. The weight loss was about 31% and may be compared to the loss of 32–45% observed with the purified material. On this basis, the reactivity of the purified material, which has already seen oxidation by HNO_3, is at least as high or higher than that of raw material.

The TG of the recovered material (Fig. 10) shows initial weight loss began at about 300 °C and continued to about 700 °C. The weight of metal oxide residues increased to 14.3%, corresponding to 11.3% metals in the original sample. The DTG is well represented ($R^2 = 0.999$) by Gaussian peaks centered at 319 °C (7%), 363 °C (29%), 406 °C (51%), 477 °C (4%), and 526 °C (13%). As before, a peak for weight gain at 421 °C indicates the catalytic metals oxidize during the TG analysis in air but not under CO_2 at 600 °C

An overlay of the DTGs for raw material before and after CO_2 oxidation (Fig. 11) shows that the post-CO_2 oxidation profile is narrower and consistent with removal

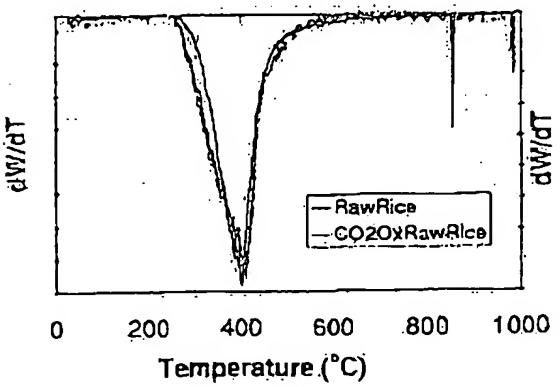

Fig. 11. DTG of rice raw material SWCNT in air before and after CO_2 oxidation.

of more easily oxidized species. The same number of peaks is used to fit both DTGs and the centers of the carbon peaks are within seven degrees or less of each other. In contrast to the complete removal of the lowest temperature peak found with the purified sample, no peak has been completely eliminated by CO_2 oxidation of the raw material. However, the distribution among the peaks has changed. The relative amount of net loss sustained by each peak was calculated by normalizing the curves based on the relative amount of metal oxide residue. A selectivity index was defined based on the normalized areas to express the amount lost by each peak relative to the total amount of carbon lost. As shown in Table 1, the first and fourth peaks are more reactive than the average, while the last peak is more resistant than the average. This confirms the initial observation that the first peak suffers the greatest relative loss while the highest temperature peak has been relatively enriched.

A HRTEM study was made of both purified and raw samples before and after CO_2 oxidation. The starting materials already have been the objects of extensive HRTEM studies [5,6]. The photographs given here confirm that our samples conform to the expected characteristics. For example, inspection of several regions of the raw material gave evidence of the variety of structures commonly associated with this sample. Fig. 12 shows bundles of SWCNTs. The nano-particulate metallic NiCo catalyst is also evident. Encasement of larger catalyst particles by graphitic carbon (not shown) was also observed. A smaller bundle of purified tubes is shown in Fig. 13. Overall, reduction in the amount of amorphous carbon adhering to the tubes is observed. Catalyst particles encased in graphitic structures are still evident.

Images of samples after CO_2 oxidation provide new information. Fig. 14 shows that the tubular structure and rope-like arrays in the purified sample have been preserved. It is also clear that the encasements of graphitic carbon about the catalyst particles also remain intact (Fig. 15). This observation is consistent with the fact that

Table 1
Selectivity of carbon removal by CO_2 oxidation of rice raw material SWCNTs

Peak temperature (°C)	Total carbon (%)		Selectivity*
	Before	After	
313–319	13.7	6.7	1.48
358–363	27.5	27.9	0.99
409–406	45.1	49.0	0.92
478–477	5.9	3.8	1.32
525–526	7.8	12.5	0.44
Metals content	5.8	11.3	

* Selectivity is the ratio of carbon lost on CO_2 oxidation for each peak relative to the total loss of carbon by the sample calculated from the increase in metals content.

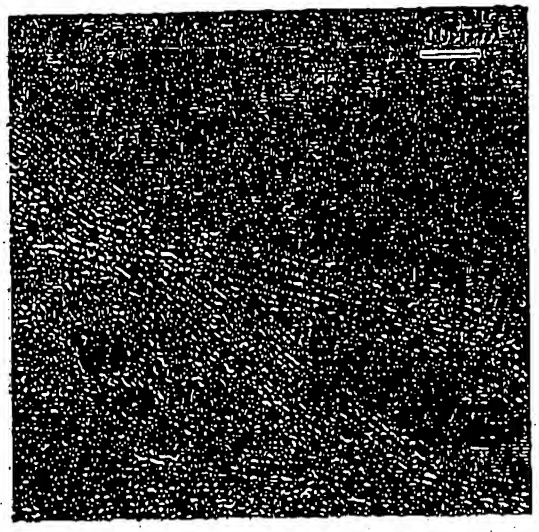

Fig. 12. High-resolution TEM of raw material.

oxidation of the metallic particles took place during the TG of the material recovered after CO_2 oxidation. An array of tubes showing evidence of damage to the SWCNT bundle is presented in Fig. 16. Views of the CO_2 oxidized raw material show similar aspects (Fig 17). In addition, it appears that some ill-defined carbon nanostructures and possibly amorphous carbon still adhere to the surface of the tubes. This again corresponds to the TG results that show CO_2 oxidation does not completely remove the low temperature peak from the raw material. In all of the images there is scant direct evidence of tube ends or open

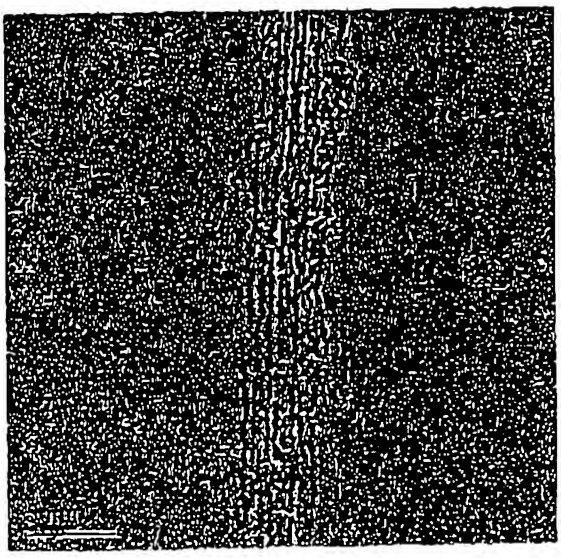

Fig. 13. High-resolution TEM of purified tubes.

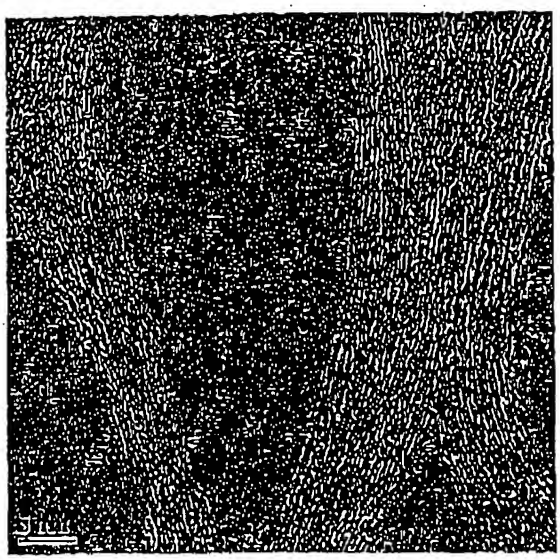

Fig. 14. High-resolution TEM of purified tubes after CO_2 oxidation at 600 °C.

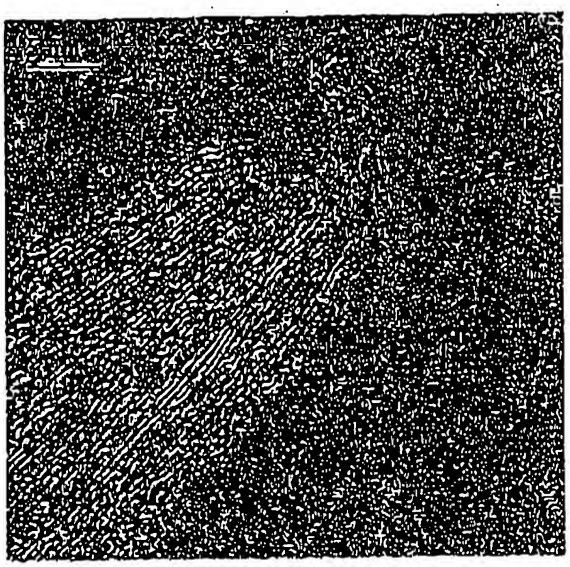

Fig. 16. High-resolution TEM of purified tubes after CO_2 oxidation at 600 °C. Note side-wall damage.

tube ends, in particular. However, tube side-wall defects are apparent. These might arise from the enlargement of small defects by oxidation. For example, the nitric acid purification leaves behind up to 5% carbon in the form of oxygenated functionalities presumed to cap the dangling bonds at defect sites [12]. These groups were removed by pyrolysis beginning at 350 °C. Significantly, the defects recreated by pyrolysis were oxidized again with ozone at a lower temperature, then thermally decomposed again to create a cycle that effectively titrated tube defects with O_2 [12]. In view of the ready decomposition of the partially oxidized sites and oxidation of the resulting defects, it is reasonable to interpret the results of CO_2 oxidation in a similar way. In addition to the amorphous carbon that is well recognized to be reactive, carbons that were partially oxidized during the nitric acid purification would also be

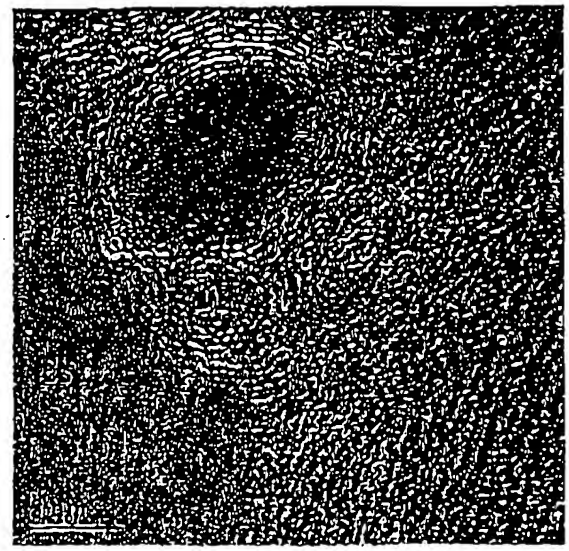

Fig. 15. High-resolution TEM of purified tubes after CO_2 oxidation at 600 °C.

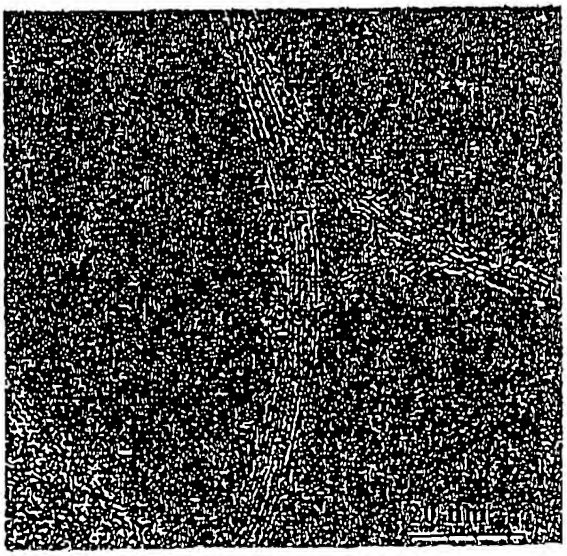

Fig. 17. High-resolution TEM of raw material after CO_2 oxidation at 600 °C.

more susceptible and thus selectively removed by CO_2 oxidation.

In this light, it is interesting to compare the samples on the basis of oxygen content. Direct oxygen determination places the samples in the order purified (13.3%)>purified, CO_2-oxidized (8.0%)>raw (4.9%). Thus, the nitric acid oxidized material has the highest oxygen content, while the doubly oxidized material stands second. This result can be understood by taking into account the loss of oxygenated groups incurred by pyrolytic mechanisms at the temperature used for secondary CO_2 oxidation.

4. Summary and conclusions

Raw and purified SWCNTs produced by the laser ablation technique were analyzed by CAPTO and TG. Both analyses (Figs. 1–5) reveal that despite the considerable extent of purification achieved by nitric acid oxidation, the purified sample remained a mixture of carbons of different oxidative reactivity. Comparative analyses were conducted in three atmospheres of differing oxidative reactivity—oxygen, air, and carbon dioxide. In each case, a progression of four to five peaks was found as the oxidation temperature increased. The major peak in each analyses was attributed to nanotubes while minor peaks were associated with amorphous carbon, graphitic shells surrounding catalysts particles, graphitic debris, or partially oxidized remnants of the nitric acid purification procedure. The oxidation temperature for each component increased as expected in going from oxygen to air to carbon dioxide. In addition, the degree of selectivity among the components was inversely proportional to the oxidative severity of the reactive atmosphere. Least discrimination was found under oxygen while most was found under carbon dioxide. Air was intermediate.

The very selective nature of the endothermic oxidation by carbon dioxide makes it a convenient preparative method for removing the most reactive components of the purified sample. Thus, 28–36% of the mass was removed from samples ranging from 60 to 200 mg by isothermal oxidation under carbon dioxide at 600 °C. Analyses of the remaining material by CAPTO (oxygen) and DTG (air) show that the initial oxidation peak had been largely removed. This peak is associated with partially oxidized remnants of amorphous carbon and nanotube fragments remaining from the prior nitric acid purification. When applied to the raw material, the CO_2 oxidation was less successful in selectively removing the most reactive component. In this case the oxidation profile was narrowed but the DTG still contained a tightly grouped series of five individual peaks.

The identification of the material removed by carbon dioxide oxidation relies on circumstantial evidence. It is evident by examination of HRTEM images taken before and after the carbon dioxide oxidation that the main body of nanotubes is preserved. The before images also are consistent with the conclusion of another TEM study that the nitric acid purification step leaves behind partially damaged tubes [6]. It is reasonable that partially damaged tubes may be more susceptible to oxidation by carbon dioxide than whole tubes and that the most extensively damaged tubes could be selectively removed from the purified sample by a controlled temperature oxidation. Selective removal is aided by the fact that the CO_2 reaction is endothermic. It has also been reported that thermal treatment promotes "healing" of the defects by skeletal rearrangements. At least some of this healing effect is achieved at 600 °C. Thus, two reactions may go on concurrently; removal of the most damaged tubes by oxidation, healing the less damaged tubes by thermolytic reactions.

No evidence was found in these experiments for effects due to local heating, ignition, or run away reactions. The TG and DTG curves (Fig. 2) display well defined features indicative of stepwise oxidation. The relative size of the low temperature component is nearly the same regardless of whether oxygen, air, or carbon dioxide was used, consistent with selective reaction of an individual component. It is especially convincing that the endothermic carbon dioxide reaction selectively removes the corresponding initial peak of the exothermic oxidations. These results support the assignment of peaks to components according to their oxidative reactivity.

Selective oxidation by carbon dioxide is a simple, clean, and reproducible method for the removal of extraneous materials from SWCNT samples. The procedure does not require complex apparatus and has the added advantage that it requires no filtration or other separation. Samples treated this way appear more uniform in their oxidative characteristics when analyzed by TG and DTG in air, or CAPTO in oxygen. This selective oxidation has a pronounced effect on the adsorption characteristics of these nanotubes [12] including the enhancement of their hydrogen storage capacity by a factor of 2–3 [13].

We also note in passing that the oxidative reactivity of carbon nanotubes has become a more intriguing aspect of their many unusual properties since the report of their ready ignition on exposure to an ordinary photo-flash [14]. Indeed, we have reproduced the reported photo ignition using the same raw material nanotube sample that was studied here [15]. Appreciation of their ready oxidation at relatively low temperatures as found above may also assist understanding of the photochemical ignition of nanotubes.

Acknowledgements

This work was performed while M.R.S. held a National Research Council–NETL Research associateship. The assistance provided by Leslie Bittner in obtaining TG data is gratefully acknowledged. Dr. J. Karl Johnson provided

helpful discussions on nanotubes. Reference in this work to any specific commercial product is to facilitate understanding and does not necessarily imply endorsement by the United States Department of Energy.

References

[1] Tsang SC, Harris PJF, Green MLH. Thinning and opening carbon nanotubes by oxidation using carbon dioxide. Nature 1993;362:520–2.

[2] Tsang SC, Harris PJF, Claridge JB, Green MLHA. Microporous carbon produced by arc-evaporation. J Chem Soc Chem Commun 1993;1519–20.

[3] Smith MR, Bittner E, Bockrath B. Hydrogen storage on carbon single-walled nanotubes. In: Carbon'01, Proceedings of the 25th International Conference on Carbon, Paper No. 36.5. Lexington, KY: American Carbon Society, 12–18 July 2001.

[4] Rinzler AG, Liu J, Dai H, Nikolaev P, Huffman CB, Rodriguez-Macias F et al. Large-scale purification of single-wall carbon nanotubes: process, product, and characterization. Appl Phys A 1998;67:29–37.

[5] Product information from tubes@rice, Houston, TX.

[6] Monthioux M, Smith BW, Burteaux B, Claye A, Fischer JE, Luzzi DE. Sensitivity of single-wall carbon nanotubes to chemical processing: an electron microscopy investigation. Carbon 2001;39:1251–72.

[7] Thess A, Lee R, Nikolaev P, Dai H, Petit P, Robert J et al. Crystalline ropes of metallic carbon nanotubes. Science 1996;273:483–7.

[8] LaCount RB, Kern DG, King WP, LaCount Jr. RB, Miltz Jr. DJ, Stewart AL et al. Advances in coal characterisation by programmed-temperature oxidation. Fuel 1993;72:1203–8.

[9] Billo EJ. Excel For Chemists. New York: Wiley–VCH, 1997.

[10] Mawhinney DB, Naumenko V, Kuznetsova A, Yates JT, Liu J, Smalley RE. Surface defect site density on single walled carbon nanotubes by titration. Chem Phys Lett 2000;324:213–6.

[11] Dillon AC, Gennett T, Jones KM, Alleman JL, Heben MJ. A simple and complete purification of single-walled carbon nanotube materials. Adv Mater 1999;11:1354–8.

[12] Bittner EW, Smith MR, Bockrath BC. Characterization of the surfaces of single-walled carbon nanotubes using alcohols and hydrocarbons: a pulse adsorption technique. Carbon 2003;41:1231–9.

[13] Smith MR, Bittner EW, Shi W, Johnson JK, Bockrath BC. Chemical activation of single-walled carbon nanotubes for hydrogen adsorption. J Phys Chem B, in press.

[14] Ajayan PM, Terrones M, de la Guardia A, Huc V, Grobert N, Wei BQ et al. Nanotubes in a flash—ignition and reconstruction. Science 2002;296:705–6.

[15] Bockrath B, Johnson JK, Sholl DS, Howard B, Matranga C, Shi W et al. Letter to the editor: igniting nanotubes with a flash. Science 2002;297:192.